Direct microbial electron uptake as a mechanism for stainless steel corrosion in aerobic environments

Zhou, Enze; Li, Feng; Zhang, Dawei; Xu, Dake; Li, Zhong; Jia, Ru; Song, Hao; Gu, Tingyue; Homborg, Axel M.; Mol, Johannes M.C.

DOI
10.1016/j.watres.2022.118553

Publication date
2022

Document Version
Final published version

Published in
Water Research

Water Research 219 (2022) 118553

Contents lists available at ScienceDirect

Water Research

journal homepage: www.elsevier.com/locate/watres

Direct microbial electron uptake as a mechanism for stainless steel corrosion in aerobic environments

Enze Zhou [a,b,c,#], Feng Li [d,#], Dawei Zhang [e,#], Dake Xu [a,b,*], Zhong Li [a,b], Ru Jia [f], Yuting Jin [a,b], Hao Song [d], Huabing Li [a], Qiang Wang [c], Jianjun Wang [a], Xiaogang Li [e], Tingyue Gu [f], Axel M. Homborg [g], Johannes M.C. Mol [h], Jessica A. Smith [i], Fuhui Wang [a], Derek R. Lovley [b]

[a] Shenyang National Laboratory for Materials Science, Northeastern University, Shenyang, 110819, China
[b] Electrobiomaterials Institute, Key Laboratory for Anisotropy and Texture of Materials (Ministry of Education), Northeastern University, Shenyang, 110819, China
[c] Key Laboratory of Electromagnetic Processing of Materials (Ministry of Education), Northeastern University, Shenyang, 110819, China
[d] Key Laboratory of Systems Bioengineering (Ministry of Education), School of Chemical Engineering and Technology, SynBio Research Platform, Collaborative Innovation Center of Chemical Science and Engineering, Tianjin University, Tianjin, 300072, China
[e] Corrosion and Protection Center, University of Science and Technology Beijing, Beijing, 100083, P. R., China
[f] Department of Chemical and Biomolecular Engineering, Institute for Corrosion and Multiphase Technology, Ohio University, Athens, Ohio, 45701, USA
[g] Netherlands Defence Academy, P.O. Box 505, 1780AM, Den Helder, the Netherlands
[h] Delft University of Technology, Department of Materials Science and Engineering, Mekelweg 2, 2628CD Delft, the Netherlands
[i] Department of Biomolecular Sciences, Central Connecticut State University, 1615 Stanley Street, New Britain, CT, 06050, USA

ARTICLE INFO

Keywords:
Microbiologically influenced corrosion
Shewanella oneidensis
Direct electron transfer
Porin-cytochrome conduit
Stainless steel

ABSTRACT

Shewanella oneidensis MR-1 is an attractive model microbe for elucidating the biofilm-metal interactions that contribute to the billions of dollars in corrosion damage to industrial applications each year. Multiple mechanisms for *S. oneidensis*-enhanced corrosion have been proposed, but none of these mechanisms have previously been rigorously investigated with methods that rule out alternative routes for electron transfer. We found that *S. oneidensis* grown under aerobic conditions formed thick biofilms (~50 μm) on stainless steel coupons, accelerating corrosion over sterile controls. H_2 and flavins were ruled out as intermediary electron carriers because stainless steel did not reduce riboflavin and previous studies have demonstrated stainless does not generate H_2. Strain Δ*mtrCBA*, in which the genes for the most abundant porin-cytochrome conduit in *S. oneidensis* were deleted, corroded stainless steel substantially less than wild-type in aerobic cultures. Wild-type biofilms readily reduced nitrate with stainless steel as the sole electron donor under anaerobic conditions, but strain Δ*mtrCBA* did not. These results demonstrate that *S. oneidensis* can directly consume electrons from iron-containing metals and illustrate how direct metal-to-microbe electron transfer can be an important route for corrosion, even in aerobic environments.

1. Introduction

Microbial corrosion is a common form of metal deterioration that negatively affects many industrial applications including petroleum pipelines, offshore platforms and ships, nuclear power plant facilities, medical instruments, and even space stations (Barravecchia et al., 2018; Huang et al., 2021; Yang et al., 2021; Zhang et al., 2022). Nearly 10–20% of total corrosion damage globally, equivalent to approximately US $250–500 billion annually, is attributed to microbial activity (Chugh et al., 2022; Skovhus et al., 2017). Although the possible role of microorganisms in corrosion was discovered over a century ago (Gaines, 1910), there still is little mechanistic information.

Current models for microbial corrosion of iron-containing metals suggest that microorganisms enhance corrosion under aerobic conditions primarily through indirect mechanisms whereas anaerobic corrosion is often more directly linked to anaerobic respiration (Jia et al., 2019; Lekbach et al., 2021; Loto, 2017; Wu et al., 2020). The key reaction in corrosion of iron-containing metals is:

$$Fe^0 \rightarrow Fe^{2+} + 2e^-$$

* Corresponding authors.
E-mail addresses: xudake@mail.neu.edu.cn (D. Xu), hsong@tju.edu.cn (H. Song).
# Equally contributed to this work.

https://doi.org/10.1016/j.watres.2022.118553
Received 23 February 2022; Received in revised form 29 April 2022; Accepted 3 May 2022
Available online 5 May 2022

Under aerobic conditions O_2 can serve as the terminal electron acceptor for Fe^0 in an abiotic reaction:

$$2Fe^0 + O_2 + 2H_2O \rightarrow 2Fe^{2+} + 4OH^-$$

Iron-oxidizing bacteria can accelerate corrosion (Chen et al., 2019; Inaba et al., 2020; Li et al., 2019; Wang et al., 2014) potentially by removing Fe^{2+},

$$4Fe^{2+} + O_2 + 2H_2O \rightarrow 4Fe^{3+} + 4OH^-$$

and making Fe^0 oxidation more thermodynamically favorable as well as generating Fe^{3+}, which can serve as an additional oxidant for abiotic Fe^0 oxidation:

$$Fe^0 + 2Fe^{3+} \rightarrow 3Fe^{2+}$$

Other indirect mechanisms for aerobic corrosion may be possible (Lekbach et al., 2021). Biofilms growing in the prescence of oxygen may consume sufficient oxygen to establish anaerobic conditions near the biofilm-metal interface (Lekbach et al., 2018; Liu et al., 2016; Qian et al., 2019; Ress et al., 2020; Yue et al., 2019). If so, then mechanisms previously proposed for microbial corrosion in anaerobic environments could be important under conditions in which the bulk environment is aerobic.

One model for corrosion under anaerobic conditons is direct electron uptake from Fe^0 to support respiration (Gu et al., 2021; Lovley, 2022; Zhou et al., 2022). Although this model is frequently invoked, direct metal-to-microbe electron transfer has only been documented for *Geobacter* species, which can oxidize Fe^0 with the reduction of fumarate, nitrate, or Fe(III) (Liang et al., 2021; Tang et al., 2019, 2021). Outer-surface, multi-heme, c-type cytochromes appear to be important electrical contacts for the metal-to-microbe electron transfer.

Alternatively, Fe^0 may reduce protons to produce H_2:

$$Fe^0 + 2H^+ \rightarrow Fe^{2+} + H_2$$

either abiotically or aided by hydrogenases (Lovley, 2022). H_2 is an effective electron shuttle between Fe^0 and microbes because it is an excellent electron donor for all forms of anaerobic respiration. It has been proposed that flavins may also function as electron shuttles for microbially enhanced corrosion (Jia et al., 2017a; Li et al., 2022; Zhang et al., 2015). In this model Fe^0 transfers electrons to flavin:

$$Fe^0 + Flavin_{oxidized} \rightarrow Fe^{2+} + Flavin_{reduced}$$

Then reduced flavin serves as the electron donor for anaerobic respiration:

$$Flavin_{reduced} + Microbe\ Electron\ Carrier_{oxidized} \rightarrow Flavin_{oxidized} + Microbe\ Electron\ Carrier_{reduced}$$

However, as recently reviewed (Lovley, 2022), the key steps of flavin reduction by the iron-containing metals under study and anaerobic respiration driven by the reduced flavins have yet to be demonstrated in corrosion studies.

Shewanella oneidensis MR-1 is an attractive model microorganism for the study of corrosion mechanisms because: it is genetically tractable; it grows aerobically and anaerobically; it grows with H_2 as the electron donor; it can oxidize reduced flavins to support respiration; and it is capable of direct electron exchange with minerals and electrodes (Fredrickson et al., 2008; Hernandez-Santana et al., 2022; Jiang et al., 2020; Ross et al., 2011; Rowe et al., 2018; Shi et al., 2016). Anaerobic corrosion via H_2 or flavins as electron shuttles as well as direct electron uptake from Fe^0 have all been proposed as potential mechanisms for corrosion by *S. oneidensis* and related species (Herrera and Videla, 2009; Jiang et al., 2020; Jin et al., 2019; Kalnaowakul et al., 2020; Li et al., 2021a, 2021b; Lutterbach et al., 2009; Miller et al., 2018; Philips et al., 2018; Schütz et al., 2015; Shi et al., 2006; Turick et al., 2002; Windt et al., 2003; Wurzler et al., 2020). However, none of the suggested mechanisms were rigorously evaluated with construction of the appropriate mutant strains or other strategies to rule out alternative mechanisms.

Therefore, we studied the mechanisms by which *S. oneidensis* corrodes stainless steel, an iron-containing metal employed in fabrication of a diversity of structures and devices (Ledezma et al., 2015; Wang et al., 2021; Yang et al., 2021). We provided evidence for direct electron uptake via a porin-cytochrome complex and demonstrated that microorganisms growing in aerobic environments can corrode metals via direct metal-to-microbe electron exchange, a finding with important implications for designing strategies for corrosion mitigation.

2. Materials and methods

2.1. Materials preparation

316 L stainless steel was obtained from the School of Metallurgy, Northeastern University, Shenyang, Liaoning, China. The major alloy components were: (wt.%) Cr 16.78%, Ni 10.50%, Mo 2.09%, Mn 1.18%, Si 0.43%, P 0.03%, C 0.02%, and Fe for balance. The sample was cut into square coupons (10 mm in length and width, 5 mm in height) and abraded with 150, 400, 600, 800, and 1000 grit abrasive papers sequentially. All coupons were cleaned in distilled water and pure ethanol for 20 min each before being air dried and sterilized under ultraviolet light for 30 min before use.

2.2. Plasmid construction, transformation, and culture conditions

All plasmid constructions were performed in *Escherichia coli* Trans T1. *E. coli* strains were cultured in Luria-Bertani (LB) medium at 37 °C with 200 rpm. Whenever needed, 50 μg/mL Kanamycin was added in the culture medium for plasmid maintenance. To benefit the multigene assembly in *S. oneidensis*, a Biobrick compatible expression vector pYYDT was adopted, which allowed various levels of gene expression upon differential isopropyl β-D-1-thiogalactopyranoside (IPTG) induction. To repress the expression levels of outer membrane "porin-cytochrome" genes *mtrA, mtrB*, and *mtrC*, a transcriptional regulation technology, i.e., clustered regularly interspaced short palindromic repeats interference (CRISPRi) was adopted as previously method (Cao et al., 2017). First, a single CRISPRi plasmid (pHG11-sgRNA-dCas9) expressing dCas9 under the control of a Ptac promoter and a sgRNA under a constitutive pCI promoter was constructed. Then, three sgRNAs (*mtrA*-NT1, *mtrB*-NT1, and *mtrC*—NT1) were designed to target the nontemplate DNA strand of the coding sequence of *mtrA, mtrB*, and *mtrC* with the nearest distance from the binding site to the transcription start site. Three CRISPRi systems (i.e., -MtrA, -MtrB, and -MtrC) were thus constructed using the Golden Gate assembly method. Furthermore, by combining the expression of sgRNAs targeting *mtrA, mtrB* and *mtrC*, the -MtrABC CRISPRi system was designed to inhibit the three *mtr* genes simultaneously. These constructed plasmids were transformed into the plasmid donor cells (*E. coli* WM3064, a DAP auxotroph), which were then transferred into *S. oneidensis* by conjugation. For the growth of *E. coli* WM3064, 0.3 mM DAP was added to the culture medium. In brief, the homology arms containing attB of *SO_0702* were amplified from genome (**Table S1**), which were then fused by overlap PCR. The fused fragment was cloned into suicide plasmid pHG1.0 using Gateway BP clonase enzyme and subsequently the resulting vectors were transferred into *S. oneidensis* via conjugation with the aid of *E. coli* DAP auxotroph WM3064. The deletion constructs into the chromosome were selected by resistance to gentamicin (15 μg/mL) and confirmed by PCR. Verified transconjugants were grown in LB in the absence of NaCl and plated on LB supplemented with 10% sucrose. Gentamicin-sensitive and sucrose-resistant colonies were screened by PCR for intended deletions and the mutants were verified by sequencing the mutated region.

2.3. Surface topography

A confocal laser scanning microscope (CLSM) (C2 Plus, Nikon, Tokyo, Japan) was also used to observe bacterial viability, biofilm distribution, and thickness by Live/Dead staining. Sessile cells attached on the coupon surfaces were counted using ImageJ software (National Institutes of Health, Bethesda, MD, USA) (Xia et al., 2015).

2.4. Electrochemical characterizations

Electrochemical tests were performed using a Gamry electrochemical workstation (Reference 600, Gamry Instruments, Warminster, PA, USA). 316 L SS coupons (10 mm × 10 mm × 5 mm) were configured as the working electrodes by embedding one coupon (1 cm^2 exposed surface) in Epoxy for each electrode, a platinum sheet (Purity, 99.99%; 10 mm × 10 mm × 0.1 mm) served as the counter electrode, and a saturated calomel electrode (SCE) was used as the reference electrode. Measurements were performed in 250 mL LB medium in the presence and absence of bacteria at 30 °C under aerobic condition. Open circuit potential (OCP) (E_{ocp}), linear polarization resistance (LPR), and electrochemical impedance spectroscopy (EIS) were carried out in sequence daily. For LPR measurements, the potential was swept from −10 mV to +10 mV (vs. E_{ocp}) with a scan rate of 0.125 mV/s. EIS was scanned at a frequency from 10^5 Hz to 10^{-2} Hz by applying a AC signal of 5 mV amplitude at the E_{ocp}. The ZSIMPWIN software (Princeton Applied Research, Oak Ridge, USA) was used to analyze the impedance data by fitting appropriate equivalent circuits (ECs). R_{ct} was obtained by EIS fitting. According to the previous report (Jin et al., 2019), the $R(QR)$ equivalent circuit model was used to fit the abiotic control EIS data and the $R(Q(R(QR)))$ equivalent circuit model was used for the biotic coupons. At the end of the 7th day, the anodic potentiodynamic polarization curves and cathodic potentiodynamic polarization curves were measured by using separate electrodes with a constant scan rate of 0.166 mV/s. Note that the Tafel slopes of cathodic polarization curves were used to determine the accurate i_{corr} values. Each electrochemical measurement was repeated at least three times using different electrochemical glass cells to verify reproducibility and the average values were reported.

Electrochemical noise (EN) was measured by a Zahner IM6 electrochemical workstation (Zahner-Elektrik, Zahner, Kronach, Germany). EN was individually measured under E_{ocp} conditions, using two nominally identical working electrodes and one SCE reference electrode. EN measurements were recorded for a total of 168 h with a data sampling interval of 0.25 s. The electrochemical cells were placed in a Faradaic cage to avoid electromagnetic disturbance from external sources. A low-pass filter of 2 Hz was applied during data recording. The maximum range of the zero resistance ammeter (ZRA) was set at 21 nA (Zhao et al., 2018). To analyze MIC induced by *S. oneidensis*, time-frequency analysis using Hilbert spectra was used to decompose the corresponding transients in the EN signals into instantaneous frequencies according to the previously reported procedures (Zhao et al., 2018). The Hilbert-Huang transform was first introduced by Huang et al. (1998). EN analysis by using Hilbert spectra of EN data was first proposed by Homborg et al. (2013).

2.5. Characterization of pitting corrosion morphology

The largest pit depths after 7 days of immersion were detected under CLSM (LSM 710, Zeiss, Jena, Germany). Corrosion products and biofilms were removed using previously reported methods (Jia et al., 2017b; Jin et al., 2019). Pit profiles, including depths and widths, were obtained from three independent coupons in the same 250 mL flask with 50 mL culture medium. For each coupon, the pits from the whole coupon surface were measured.

2.6. Quantification of riboflavin

Riboflavin secreted by each strain was measured using high performance liquid chromatography (UltiMate 3000, Thermo Scientific, Waltham, MA, USA) according to previous reports (Jin et al., 2019; Liu et al., 2017). Cultures were centrifuged and filtered (pore size 0.22 μm) and then subjected to a reverse-phase column (4.6 × 150 mm, 5 μm C18, Bonna-Agela Technologies, Tianjin, China). Methanol and 0.05 M ammonium acetate (pH 6.0, 15:85 v/v) were used as the mobile phase. Riboflavin was separated with a linear gradient at a flow rate of 600 μL/min with 20 μL injection volume using the following method: 15:85 v/v to 30:70 v/v for 1.5 min, followed by 30:70 v/v to 85:15 v/v for 2.5 min, isocratic 85:15 v/v for 4 min, and linear gradient to 15:85 v/v for 1.5 min, and finally isocratic 15:85 v/v for 6.5 min.

The oxidized riboflavin concentration was spectrophotometrically measured at 445 nm (Arsalan et al., 2020; Edelmann et al., 2019; Kim et al., 2020; Mikhailova et al., 2015). Throughout the experimental period, an anaerobic NaCl (10 g/L) solution with or without 316 L SS coupons was used. The culture medium was deoxygenated by filter-sterilized N_2 gas bubbling for at least 0.5 h prior to use. The standard curve of oxidized riboflavin concentration was obtained from **Fig. S1a**. When reducing agent Na_2SO_3 was added, the oxidized riboflavin at 445 nm would be reduced (**Fig. S1b**).

2.7. Dissolved oxygen concentration measurement

S. oneidensis biofilms grown on LB agar plates at 30 °C for two days were used to measure the concentration of oxygen beneath the biofilm. A Unisense oxygen microsensor (OX-5, Unisense A/S, Aarhus, Denmark) with a 5 μm tip diameter was used. The oxygen microsensor was calibrated based on the instructions provided by the manufacturer. The sensor was measured at a step size of 3 μm, a measuring period of 1 s, and a waiting time of 3 s between measurements. The SensorTrace Profiling software was used to analyze the data.

2.8. Iron ion release

Three coupons were exposed to 50 mL LB culture medium, either with or without different *S. oneidensis* strains at 30 °C for 7 days. After immersion, concentrations of iron ions in the culture medium were measured by a flame atomic absorption spectrophotometer (Model Z-2300, Hitachi, Tokyo, Japan). Each experiment was repeated three times.

2.9. Planktonic cell number

Planktonic cells in the LB culture medium after incubation with different *S. oneidensis* strains were counted using a hemocytometer. An optical microscope at 400X magnification was used to quantify the planktonic cells.

2.10. Anaerobic corrosion tests

LPR measurement was used to evaluate the corrosion rate of 316 L SS coupons in the presence and absence of bacteria in the LB culture medium. To obtain the reduction rate of nitrate, 316 L SS coupons were first cultured in LB medium with these strains for three days to develop mature biofilms. Then the coupons were transferred to an anaerobic medium with NaCl (10 g/L) and nitrate (10 mM). The culture medium was deoxygenated by filter-sterilized N_2 gas bubbling for at least 0.5 h prior to use.

3. Results and discussion

3.1. Corrosion of stainless steel under aerobic conditions

S. oneidensis grown in aerobic medium colonized stainless steel coupons, forming thick biofilms (47 ± 14 μm, cell density 6.7 ± 0.5 × 10^7 cells/cm^2, n = 3) within 7 days (Fig. 1a). Multiple analyses demonstrated that corrosion was substantially accelerated in the presence of *S. oneidensis* versus sterile medium (Fig. 2). This included a decrease in linear polarization resistance (R_p), which is inversely proportional to corrosion rate (Fig. 2a), as well as lower charge transfer resistance (R_{ct}), which reflects the resistance to electron transfer between the metal surface and biofilm (Fig. 2b and **Table S2**). Biofilm growth was associated with a negative shift in corrosion potential (E_{corr}) and increased corrosion current density (i_{corr}), further indicating higher corrosion activity (Fig. 2c). X-ray diffraction of the coupon surfaces after 7 days of immersion in medium identified $Fe_{6.6}Cr_{1.7}Ni_{1.2}Si_{0.2}Mo_{0.1}$ as the only corrosion product in both the sterile and inoculated samples (**Fig. S2**).

3.2. Lack of corrosion via electron shuttling

H_2 could be ruled out as a potential electron shuttle intermediary for the enhanced corrosion in the presence of *S. oneidensis* because stainless steel does not abiotically produce H_2 at cirumneutral pH (Tang et al., 2021). To determine whether flavins might function as an electron shuttle, oxidized riboflavin was added to stainless steel in the absence of cells. The riboflavin was not reduced, even after extended incubation (**Fig. S3**). Thus, the first step in electron shuttling, electron transfer to the shuttle, is hindered, making electron shuttling via flavin unlikely. An alternative potential function for riboflavin is as a co-factor to enhance the electron transfer effectiveness of the porin-cytochrome conduit in *S. oneidensis* (Okamoto et al., 2014; Xu et al., 2016).

3.3. Deleting the MtrCBA porin-cytochrome conduit inhibits corrosion

The porin-cytochrome conduit comprised of the inner-facing multiheme cytochrome MtrA, the barrel-porin protein MtrB and the multiheme outer environment-facing cytochrome MtrC is a major route for extracellular electron exchange across the outer membrane of *S. oneidensis* (Leung et al., 2021; Xie et al., 2021; Zhou et al., 2022). Deleting the genes for all three porin-cytochrome components (strain Δ*mtrCBA*) had no impact on the growth of planktonic cells, but there were fewer cells of strain Δ*mtrCBA* than the wild-type on the stainless steel (Fig. 1). Each of the electrochemical assessments of corrosion demonstrated that strain Δ*mtrCBA* corroded the stainless steel less than the wild-type strain (Fig. 2).

The open circuit potential (OCP) is a thermodynamic parameter that indicates the tendency of electron uptake by *S. oneidensis*. A more negative (lower) OCP indicates a higher thermodynamic tendency for the stainless steel working electrode to lose electrons (i.e., to be corroded). After 3 days, E_{ocp} values were lowest for coupons exposed to wild-type *S. oneidensis*, whereas values for Δ*mtrCBA* strain were between those of wild-type and sterile control (Fig. 2f).

Electrochemical noise can distinguish and quantify metastable pitting and stable pitting better than traditional electrochemical techniques. The Hilbert-Huang spectrum derived from the electrochemical noise raw data was analyzed to further elucidate the extent and type of corrosion (Fig. 3 and **Fig. S4, Fig. S5**). After three days, pitting corrosion initiated in the sterile control medium, but core pits did not form and transient amplitudes remained limited. In the incubation with wild-type *S. oneidensis*, incipient pitting corrosion was observed on the third day, which developed to stable localized corrosion after 5 days. The raw data for wild-type *S. oneidensis* showed pitting transients with amplitudes in the order of more than 120 nA after 5 days of immersion whereas the maximum amplitudes for the strain Δ*mtrCBA* were 20 nA. Artefacts reduced the overall dynamic range of the time-frequency information in the Hilbert spectra, but their characteristics indicated stable pitting kinetics, with local maxima around 10^{-2} Hz. On the 7th day, a few fast

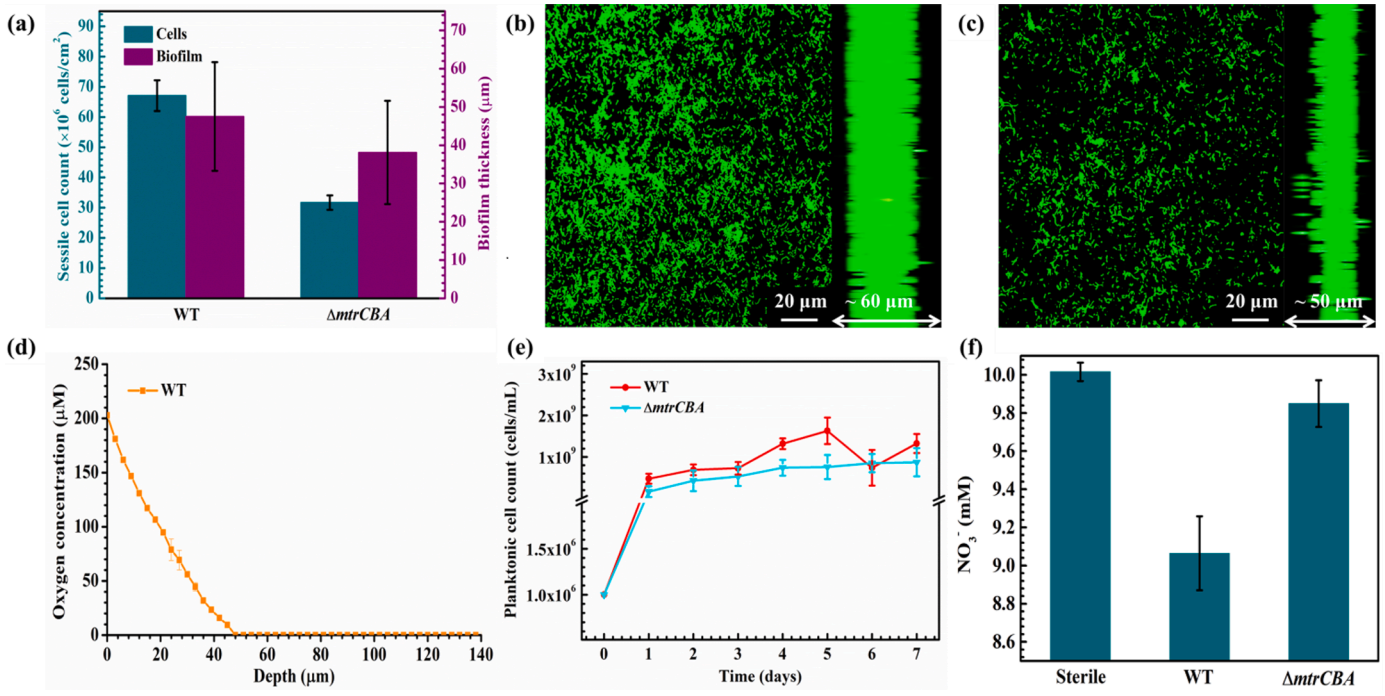

Fig. 1. Biofilms, sessile cell counts, oxygen concentrations, planktonic cell counts and NO_3^- concentrations for *S. oneidensis* strains. a Sessile cell counts and thicknesses of biofilms on 316 L SS coupon surfaces after 7 days of incubation. b CLSM image of wild-type *S. oneidensis* MR-1 strain. c CLSM image of *ΔmtrCBA* strain. d Oxygen concentration throughout layers of wild-type *S. oneidensis* MR-1 strain biofilm. e Planktonic cell counts throughout the 7-day incubation with 316 L SS coupons. f NO_3^- concentrations throughout the 7-day incubation with 316 L SS coupons.

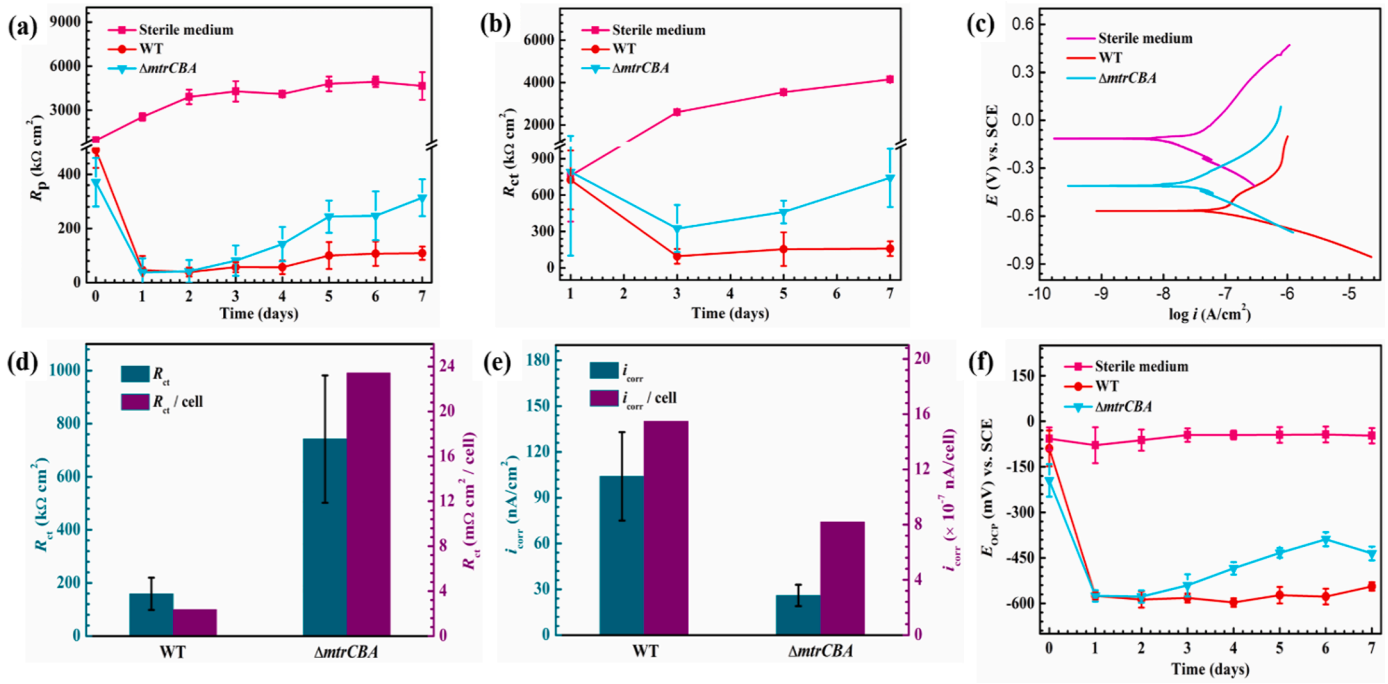

Fig. 2. Corrosion rates and normalized corrosion rates for various strains of *S. oneidensis*. a R_p data over time for 316 L SS coupons incubated in either sterile LB medium or medium containing one of the two strains of *S. oneidensis*. b Variations in R_{ct} over time. c Potentiodynamic polarization curves measured after 7 days of incubation. d R_{ct} data obtained from EIS measurements and normalized R_{ct} against sessile cell numbers on the working electrodes after 7 days of incubation. e Corrosion current density (i_{corr}) obtained from potentiodynamic polarization curves and i_{corr} normalized against sessile cell numbers. f Variations in E_{OCP} over time for 316 L SS coupons incubated in LB medium with or without various strains of *S. oneidensis*. Error bars represent standard deviations from at least three independent coupons in different electrochemical glass cells.

transient amplitudes below 10^{-1} Hz of the Hilbert spectra in the sterile medium represented pit initiation, which might turn into metastable growth that were then passivated (Zhao et al., 2018). In the presence of wild-type *S. oneidensis* strain, the transient amplitudes noticeably increased and lasted much longer, which confirmed the fact that the metastable pitting corrosion turned into stable localized corrosion by wild-type *S. oneidensis*. The Hilbert spectra of samples with the *ΔmtrCBA* strain showed nearly no obvious transients, the pitting corrosion might initiate briefly, and then the pits were passivated (Fig. 3). Direct observation of pitting depths was consistent with the electrochemical noise results. Deleting the genes for the porin-cytochrome conduit reduced stainless steel pitting (Fig. 4 and **Fig. S6**).

The finding that deleting the main porin-cytochrome conduit, which is known to facilitate extracellular electron exchange (Gong et al., 2020; Leung et al., 2021), inhibited *S. oneidensis* corrosion suggested that corrosion was linked to direct electron uptake from stainless steel. The fact that the pH of the medium was the same (pH 8.8) for the wild-type and Δ*mtrCBA* strain ruled out the possibility that the difference in corrosion rates was the result of changes in pH (**Fig. S7**).

Oxygen profiles of biofilms growing on agar indicated that it was likely that oxygen would be depleted deep within the biofilms near the stainless steel surface (Fig. 1d). Therefore, the potential role of the porin-cytchrome conduit in corrosion under anaerobic conditions was evaluated with nitrate as the electron acceptor. Biofilms were grown on stainless steel under aerobic conditions and then the stainless steel coupons were transferred into anaerobic medium with the stainless steel as the sole electron donor and nitrate as the electron acceptor. Biofilms of wild-type cells readily reduced nitrate, but strain Δ*mtrCBA* reduced nitrate much slower, if at all (Fig. 1f). This result indicated that the porin-cytochrome conduit was an important route for electron uptake from stainless steel to support nitrate reduction. Linear polarization resistance analysis further confirmed that stain Δ*mtrCBA* was much less corrosive than the wild-type under nitrate-reducing conditions (**Fig. S8**). These results further indicated that electron uptake via the porin-cytochrome conduit was an important mechanism for stainless steel corrosion.

3.4. The outer surface cytochrome OmcA is not required for corrosion

The *S. oneidensis* multi-heme *c*-type cytochrome OmcA has the potential to provide additional surface for electrical contact between the outer-surface of the cell and electron donors or acceptors, presumably by interacting with the porin-cytochrome system (Lovley and Holmes, 2022; Shi et al., 2016). However, a strain in which *omcA* was deleted was as corrosive as wild-type cells. Linear polarization resistanceanalysis demonstrated that both the wild-type and Δ*omcA* strains had a similar R_p of approximately 120 kΩ cm^2 (Fig. 5a). The E_{corr} and i_{corr} values of Δ*omcA* were also comparable to those for the wild-type (Fig. 5, **Fig. S9**). Also, the concentration of iron ions released from 316 L SS coupons after the 7-day incubation was similar for both the wild-type and Δ*omcA* samples (**Fig. S10**).

4. Implications

The results indicate that *S. oneidensis* can directly extract electrons from iron-containing metals to promote corrosion. Although the possibility of direct metal-to-microbe electron transfer with *S. oneidensis* was previously inferred (Jin et al., 2019; Li et al., 2021b; Philips et al., 2018), this inference relied on the known ability of *S. oneidensis* to exchange electrons with extracellular electron donors or acceptors, rather than any direcrt experimental evidence. Furthermore, many of the previous studies on *S. oneidensis* corrosion were conducted with iron forms, such as pure Fe^0 or carbon steel, that are likely to generate H_2 as an intermediary electron carrier for corrosion (Miller et al., 2018; Schütz et al., 2015; Windt et al., 2003). The use of stainless steel eliminated the possibility of H_2 production. The substantial decrease in corrosion and nitrate reduction when the MtrCBA porin cytochrome conduit was eliminated further demonstratred that H_2 was not an important shuttle

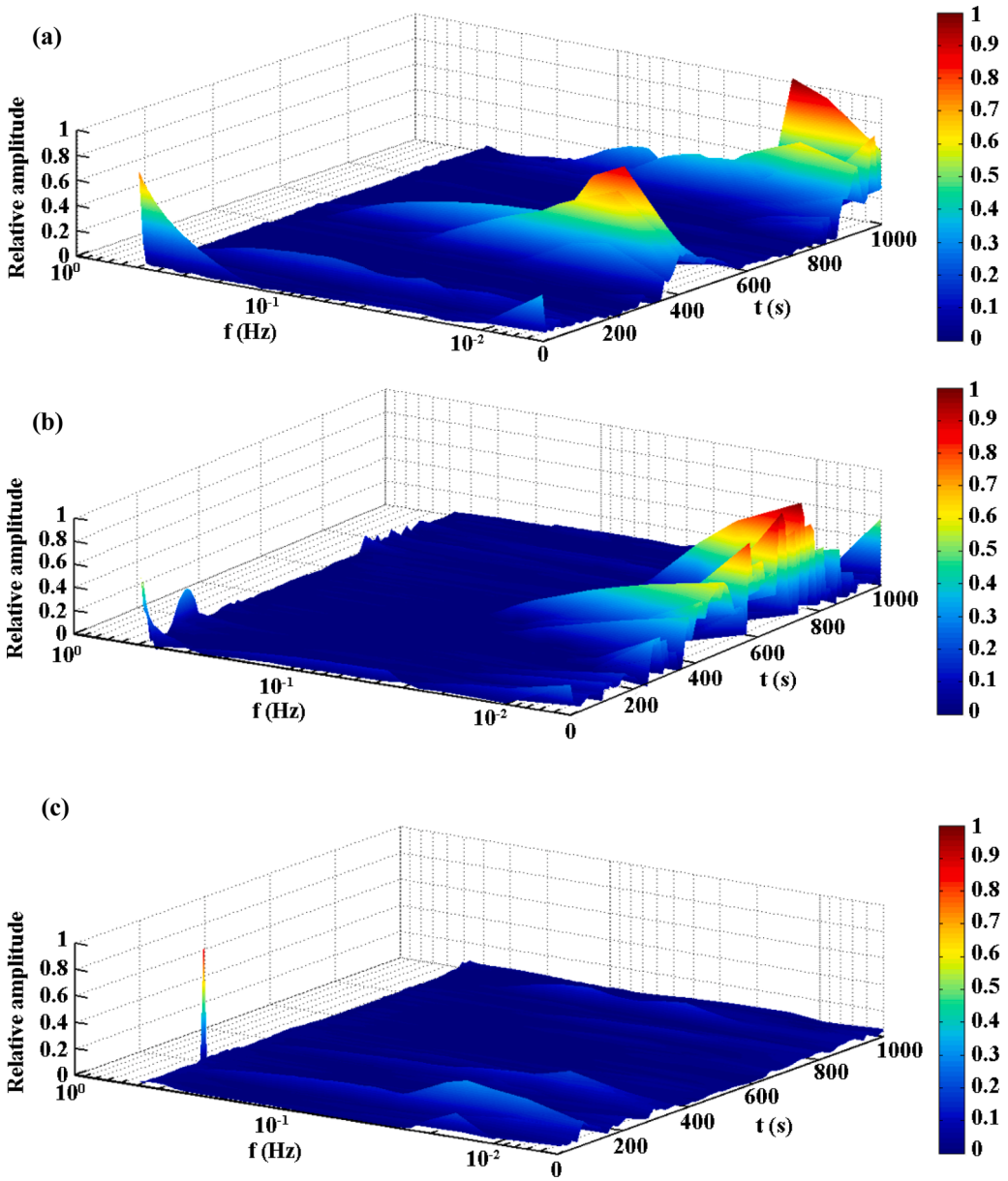

Fig. 3. Representative Hilbert spectra after immersion for 7 days. a in sterile LB medium. b Day 7 in wild-type *S. oneidensis* MR-1 strain inoculated medium. c in *ΔmtrCBA* strain inoculated medium.

for corrosion. The finding that stainless steel did not reduce riboflavin indicated that flavins were not electron shuttles for electron transfer from the stainless steel to *S. oneidensis*. However, the Δ*mtrCBA* mutant still retained some capacity for electron uptake from stainless steel, suggesting that additional porin-cytochrome systems (Beblawy et al., 2018; Golitsch et al., 2013) or other systems for extracellular electron exchange (Rowe et al., 2021; Schuetz et al., 2009) contributed to electron uptake.

Although direct electron uptake from iron-containing metals was previously demonstrated with *Geobacter* species (Liang et al., 2021; Tang et al., 2019, 2021), the studies reported here are the first to suggest a role for direct metal-to-microbe electron transfer during microbial growth in an aerobic environment. The development of anerobic conditions within aerobically grown *S. onenedensis* biofilms can induce the expression of porin-cytochrome conduits in cells within anaerobic zones (Teal et al., 2006), enhancing the possibility of metal-microbe electron exchange. As biofilm thickness increases, the consumption of organic substrates near the outer surface of the biofilms reduces the availability of organic electron donors near the stainless-steel interface. Under these conditions Fe^0 may become an important electron donor. Electron shuttles, such as flavins, may facilitate continued Fe^0-based respiration by transporting electrons from microbes within anaerobic zones to aerobic zones, in a manner similar to that proposed for phenazine-based electron transfer to oxygen in *Pseudomonas aeruginosa* biofilms (Saunders et al., 2020). Under these conditions oxygen is the ultimate electron acceptor for the electrons that *S. onedensis* consumes from Fe^0 oxidation.

Mechanisms for *S. oneidensis* corrosion of iron-containing metals that are more reactive than stainless steel may be more complex. Pure Fe° can generate H_2 (Philips et al., 2018; Tang et al., 2019). Fe^0 and other metals, such as carbon steel, might also reduce flavins, which could then serve as an electron shuttle for corrosion. These considerations, and the abundance of tools for genetic manipulation, suggest that *S. oneidensis* will be an excellent model for further investigations on direct microbe-to-metal electron transfer and other routes for microbial corrosion under aerobic conditions. The findings from such studies could also aid in better understanding how *S. oneidensis* consumes electrons

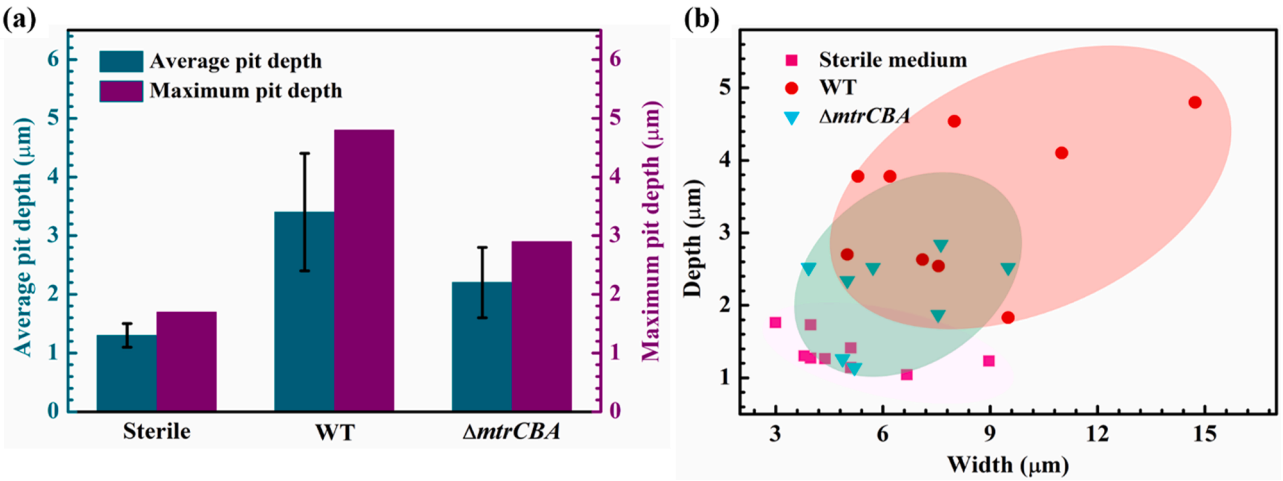

Fig. 4. Pitting caused by *S. oneidensis* biofilms. a Maximum and average pit depths on 316 L SS coupon surfaces after 7 days of immersion in either sterile LB medium or LB medium inoculated with one of the two strains of *S. oneidensis*. b Depth and width of pits observed on 316 L SS coupon surfaces after immersion in either sterile LB medium or LB medium inoculated with one of the two strains of *S. oneidensis*. Error bars represent standard deviations of three independent coupons from the same vessels.

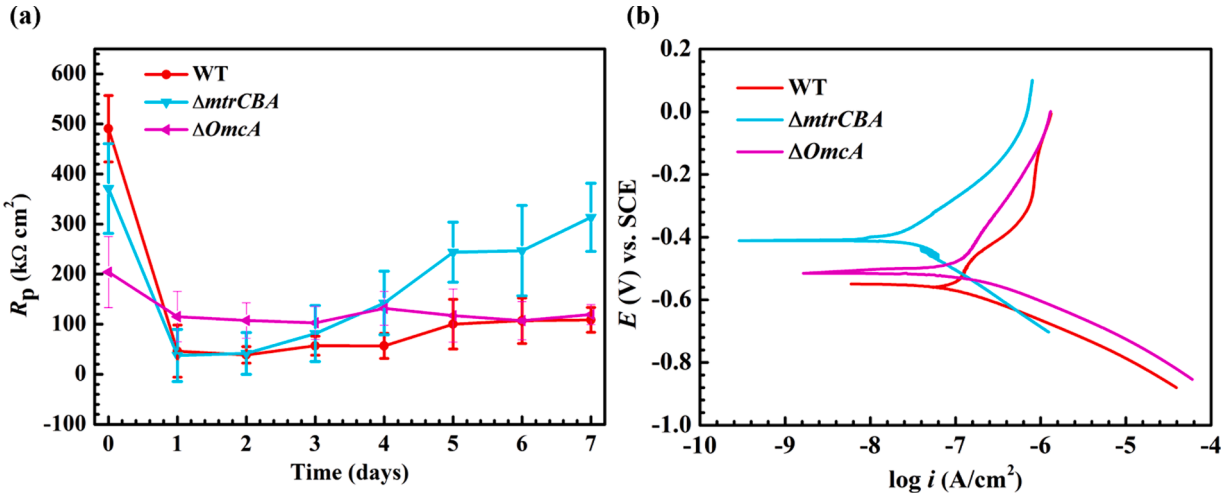

Fig. 5. Electrochemical analysis of OmcA-deficient strain of *S. oneidensis* after 7 days of incubation with 316 L SS coupons. a Variations in R_p over time after incubating different strains of *S. oneidensis* in LB medium with 316 L SS coupons, b Potentiodynamic polarization curves measured after 7 days of incubation. Error bars represent standard deviations from at least three replicating electrochemical glass cells.

from other extracellular sources, such as electrodes in bio-electrochemical technologies (Liu et al., 2012; Rowe et al., 2018; Schuetz et al., 2009).

Stainless steel is widely used in various water systems such as marine water, wastewater and water injection systems, where corrosion is common. The finding that a porin-cytochrome conduit, a common feature of many electroactive microorganisms, is associated with electron uptake provides a useful molecular target to hunt for such corrosive bacteria. Thus, this study potentially provides guidance for the detection of microbial corrosion in various water systems.

5. Conclusions

In this study, we used an interdisciplinary approach to demonstrate that direct electron uptake through a porin cytochrome conduit, an extracellular electron exchange mechanism typically associated with anaerobic respiration, can be an important mechanism for stainless steel corrosion in aerobic environments. The direct electron uptake mechanism significantly differs from previously documented routes for corrosion under aerobic conditions. Our discovery of a previously unrecognized route for metal corrosion under aerobic conditions provides new insights into the ecology of metal-corroding biofilms likely to be important in guiding the development of new corrosion mitigation strategies.

Declaration of Competing Interest

The authors declare that they have no known competing financial interests or personal relationships that could have appeared to influence the work reported in this paper.

Acknowledgements

This work was financially supported by the National Natural Science Foundation of China (U2006219), the National Key Research and Development Program of China (2020YFA0907300), the Fundamental Research Funds for the Central Universities of the Ministry of Education of China (Nos. N2102009 and N2002019) and Liaoning Revitalization Talents Program (No. XLYC1907158).

Supplementary materials

Supplementary material associated with this article can be found, in the online version, at doi:10.1016/j.watres.2022.118553.

References

Arsalan, A., Qadeer, K., Ali, S.A., Ahmed, S., Khan, R.A., Sheraz, M.A., Hassan, S., Ahmad, I., 2020. The effect of albumin in photostabilization of riboflavin: a kinetic study. J. Photoch. Photobio. A. 394, 112456.

Barravecchia, I., Cesari, C.D., Pyankova, O.V., Scebba, F., Mascherpa, M.C., Vecchione, A., Tavanti, A., Tedeschi, L., Angeloni, D., 2018. Pitting corrosion within bioreactors for space cell-culture contaminated by *Paenibacillus glucanolyticus*, a case report. Microgravity Sci. Technol. 30, 309–319.

Beblawy, S., Bursac, T., Paquete, C., Louro, R., Clarke, T.A., Gescher, J., 2018. Extracellular reduction of solid electron acceptors by *Shewanella oneidensis*. Mol. Microbiol. 109, 571–583.

Cao, Y., Li, X., Li, F., Song, H., 2017. CRISPRi-sRNA: transcriptional-translational regulation of extracellular electron transfer in *Shewanella oneidensis*. ACS Synth. Biol. 6, 1679–1690.

Chen, S., Deng, H., Liu, G., Zhang, D., 2019. Corrosion of Q235 carbon steel in seawater containing *Mariprofundus ferrooxydans* and *Thalassospira* sp. Front. Microbiol. 10, 936.

Chugh, B., SheetalSingh, M., Thakur, S., Pani, B., Singh, A.K., Saji, V.S., 2022. Extracellular electron transfer by *Pseudomonas aeruginosa* in biocorrosion: a review. ACS Biomater. Sci. Eng. 8, 1049–1059.

Edelmann, M., Aalto, S., Chamlagain, B., Kariluoto, S., Piironen, V., 2019. Riboflavin, niacin, folate and vitamin B12 in commercial microalgae powders. J. Food. Compos. Anal. 82, 103226.

Fredrickson, J.K., Romine, M.F., Beliaev, A.S., Auchtung, J.M., Driscoll, M.E., Gardner, T. S., Nealson, K.H., Osterman, A.L., Pinchuk, G., Reed, J.L., Rodionov, D.A., Rodrigues, J.L.M., Saffarini, D.A., Serres, M.H., Spormann, A.M., Zhulin, I.B., Tiedje, J.M., 2008. Towards environmental systems biology of *Shewanella*. Nat. Rev. Microbiol. 6, 592–603.

Gaines, R.H., 1910. Bacterial activity as a corrosive influence in the soil. J. Ind. Eng. Chem. 2, 128–130.

Golitsch, F., Bucking, C., Gescher, J., 2013. Proof of principle for an engineered microbial biosensor based on *Shewanella oneidensis* outer membrane protein complexes. Biosens. Bioelectron. 47, 285–291.

Gong, Z., Yu, H., Zhang, J., Li, F., Song, H., 2020. Microbial electro-fermentation for synthesis of chemicals and biofuels driven by bi-directional extracellular electron transfer. Syn Syst Biotechno 5, 304–313.

Gu, T., Wang, D., Lekbach, Y., Xu, D., 2021. Extracellular electron transfer in microbial biocorrosion. Curr. Opin. Electroche. 29, 100763.

Hernandez-Santana, A., Kokbudak, H.N., Nanny, M.A., 2022. The influence of iron-binding ligands in the corrosion of carbon steel driven by iron-reducing bacteria. npj Mater. Degrad. 6, 12.

Herrera, L.K., Videla, H.A., 2009. Role of iron-reducing bacteria in corrosion and protection of carbon steel. Int. Biodeter. Biodegr. 63, 891–895.

Homborg, A.M., van Westing, E.P.M., Tinga, T., Zhang, X., Oonincx, P.J., Ferrari, G.M., de Wit, J.H.W., Mol, J.M.C., 2013. Novel time–frequency characterization of electrochemical noise data in corrosion studies using Hilbert spectra. Corros. Sci. 66, 97–110.

Huang, N.E., Shen, Z., Long, S.R., Wu, M.C., Shih, H.H., Zheng, Q., Yen, N.-.C., Tung, C. C., Liu, H.H., 1998. The empirical mode decomposition and the Hilbert spectrum for nonlinear and non-stationary time series analysis. Proc. R. Soc. A. 454, 903–995.

Huang, Y., Xu, D., Huang, L., Lou, Y., Muhadesi, J.B., Qian, H., Zhou, E., Wang, B., Li, X. T., Jiang, Z., Liu, S.J., Zhang, D., Jiang, C.Y., 2021. Responses of soil microbiome to steel corrosion. npj Biofilms Microbiomes 7, 1–13.

Inaba, Y., West, A.C., Banta, S., 2020. Enhanced microbial corrosion of stainless steel by *Acidithiobacillus ferrooxidans* through the manipulation of substrate oxidation and overexpression of rus. Biotechnol. Bioeng. 117, 3475–3485.

Jia, R., Unsal, T., Xu, D., Lekbach, Y., Gu, T., 2019. Microbiologically influenced corrosion and current mitigation strategies: a state of the art review. Int. Biodeter. Biodegr. 137, 42–58.

Jia, R., Yang, D., Xu, D., Gu, T., 2017a. Electron transfer mediators accelerated the microbiologically influence corrosion against carbon steel by nitrate reducing *Pseudomonas aeruginosa* biofilm. Bioelectrochemistry 118, 38–46.

Jia, R., Yang, D., Xu, J., Xu, D., Gu, T., 2017b. Microbiologically influenced corrosion of C1018 carbon steel by nitrate reducing *Pseudomonas aeruginosa* biofilm under organic carbon starvation. Corros. Sci. 127, 1–9.

Jiang, Z., Shi, M., Shi, L., 2020. Degradation of organic contaminants and steel corrosion by the dissimilatory metal-reducing microorganisms *Shewanella* and *Geobacter* spp. Int. Biodeter. Biodegr. 147, 104842.

Jin, Y., Li, Z., Zhou, E., Lekbach, Y., Xu, D., Jiang, S., Wang, F., 2019. Sharing riboflavin as an electron shuttle enhances the corrosivity of a mixed consortium of *Shewanella oneidensis* and *Bacillus licheniformis* against 316 L stainless steel. Electrochim. Acta. 316, 93–104.

Kalnaowakul, P., Xu, D., Rodchanarowan, A., 2020. Accelerated corrosion of 316 L stainless steel caused by *Shewanella algae* biofilms. ACS Appl. Bio. Mater. 3, 2185–2192.

Kim, E., Kim, M.H., Song, J.H., Kang, C., Park, W.H., 2020. Dual crosslinked alginate hydrogels by riboflavin as photoinitiator. Int. J. Biol. Macromol. 154, 989–998.

Ledezma, P., Donose, B.C., Freguia, S., Keller, J., 2015. Oxidised stainless steel: a very effective electrode material for microbial fuel cell bioanodes but at high risk of corrosion. Electrochim. Acta. 158, 356–360.

Lekbach, Y., Liu, T., Li, Y., Moradi, M., Dou, W., Xu, D., Smith, J.A., Lovley, D.R., 2021. Microbial corrosion of metals: the corrosion microbiome. Adv. Microb. Physiol. 78, 317–390.

Lekbach, Y., Xu, D., El Abed, S., Dong, Y., Liu, D., Khan, M.S., Ibnsouda Koraichi, S., Yang, K., 2018. Mitigation of microbiologically influenced corrosion of stainless steel in the presence of *Pseudomonas aeruginosa* by Cistus ladanifer leaves extract. Int. Biodeter. Biodegr. 133, 159–169, 304 L.

Leung, D.H.L., Lim, Y.S., Uma, K., Pan, G.T., Lin, J.H., Chong, S., Yang, T.C.K., 2021. Engineering *S. oneidensis* for performance improvement of microbial fuel cell—A mini review. Appl. Biochem. Biotechnol. 193, 1170–1186.

Li, J., Du, C., Liu, Z., Li, X., 2022. Extracellular electron transfer routes in microbiologically influenced corrosion of X80 steel by *Bacillus licheniformis*. Bioelectrochemistry 145, 108074.

Li, Z., Chang, W., Cui, T., Xu, D., Zhang, D., Lou, Y., Qian, H., Song, H., Mol, A., Cao, F., Gu, T., Li, X., 2021a. Adaptive bidirectional extracellular electron transfer during accelerated microbiologically influenced corrosion of stainless steel. Commun. Mater. 2, 1–9.

Li, Z., Wang, J., Dong, Y., Xu, D., Zhang, X., Wu, J., Gu, T., Wang, F., 2021b. Synergistic effect of chloride ion and *Shewanella algae* accelerates the corrosion of Ti-6Al-alloy. J. Mater. Sci. Technol. 71, 177–185, 4 V.

Li, Z., Wan, H., Song, D., Liu, X., Li, Z., Du, C., 2019. Corrosion behavior of X80 pipeline steel in the presence of *Brevibacterium halotolerans* in Beijing soil. Bioelectrochemistry 126, 121–129.

Liang, Y., Lu, Q., Liang, Z., Liu, X., Fang, W., Liang, D., Kuang, J., Qiu, R., He, Z., Wang, S., 2021. Substrate-dependent competition and cooperation relationships between *Geobacter* and *Dehalococcoides* for their organohalide respiration. ISME Commun 1, 1–8.

Liu, H., Gu, T., Zhang, G., Cheng, Y., Wang, H., Liu, H., 2016. The effect of magneticfield on biomineralization and corrosion behavior of carbon steel induced by iron-oxidizing bacteria. Corros. Sci. 102, 93–102.

Liu, H., Matsuda, S., Hashimoto, K., Nakanishi, S., 2012. Flavins secreted by bacterial cells of *Shewanella* catalyze cathodic oxygen reduction. ChemSusChem 5, 1054–1058.

Liu, Y., Ding, M., Ling, W., Yang, Y., Zhou, X., Li, B.Z., Chen, T., Nie, Y., Wang, M., Zeng, B., 2017. A three-species microbial consortium for power generation. Energy Environ. Sci. 10, 1600–1609.

Loto, C.A., 2017. Microbiological corrosion: mechanism, control and impact—A review. Int. J. Adv. Manuf. Technol. 92, 4241–4252.

Lovley, D.R., 2022. Electrotrophy: other microbial species, iron, and electrodes as electron donors for microbial respirations. Bioresource Technol 345, 126553.

Lovley, D.R., Holmes, D.E., 2022. Electromicrobiology: the ecophysiology of phylogenetically diverse electroactive microorganisms. Nat. Rev. Microbiol. 20, 5–19.

Lutterbach, M.T., Contador, L.S., Oliveira, A.L., Galvão, M.M., de França, F.P., de Souza Pimenta, G., 2009. Iron sulfide production by *Shewanella* strain isolated from black powder. Corrosion. 2009 09391.

Mikhailova, R., Semashko, T., Demeshko, O., Ramanaviciene, A., Ramanavicius, A., 2015. Effect of some redox mediators on FAD fluorescence of glucose oxidase from *Penicillium adametzii* LF F-2044.1. Enzyme Microb. Tech. 72, 10–15.

Miller, R.B., Lawson, K., Sadek, A., Monty, C.N., Senko, J.M., 2018. Uniform and pitting corrosion of carbon steel by *Shewanella oneidensis* MR-1 under nitrate-reducing conditions. Appl. Environ. Microbiol. 84, 00790-18.

Okamoto, A., Kalathil, S., Deng, X., Hashimoto, K., Nakamura, R., Nealson, K.H., 2014. Cell-secreted flavins bound to membrane cytochromes dictate electron transfer reactions to surfaces with diverse charge and pH. Sci. Rep. 4, 5628.

Philips, J., Driessche, N.V.den, Paepe, K.D., Prévoteau, A., Gralnick, J.A., Arends, J.B.A., Rabaey, K., 2018. A novel *Shewanella* isolate enhances corrosion by using metallic iron as the electron donor with fumarate as the electron acceptor. Appl. Environ. Microbiol. 84 e01154-18.

Qian, H., Ju, P., Zhang, D., Ma, L., Hu, Y., Li, Z., Huang, L., Lou, Y., Du, C., 2019. Effect of dissolved oxygen concentration on the microbiologically influenced corrosion of Q235 carbon steel by halophilic archaeon *Natronorubrum tibetense*. Front. Microbiol. 10, 844.

Ress, J., Monrrabal, G., Díaz, A., Pérez-Pérez, J., Bastidas, J.M., Bastidas, D.M., 2020. Microbiologically influenced corrosion of welded AISI 304 stainless steel pipe in well water. Eng. Fail. Anal. 116, 104734.

Ross, D.E., Flynn, J.M., Baron, D.B., Gralnick, J.A., Bond, D.R., 2011. Towards electrosynthesis in *shewanella*: energetics of reversing the mtr pathway for reductive metabolism. PLoS ONE 6, e16649.

Rowe, A.R., Rajeev, P., Jain, A., Pirbadian, S., Okamoto, A., Gralnick, J.A., Elnaggar, M. Y., Nealson, K.H., 2018. Tracking electron uptake from a cathode into *Shewanella* cells: implications for energy acquisition from solid-substrate electron donors. MBio 9, e02203–e02217.

Rowe, A.R., Salimijazi, F., Trutschel, L., Sackett, J., Adesina, O., Anzai, I., Kugelmass, L. H., Baym, M.H., Barstow, B., 2021. Identification of a pathway for electron uptake in *Shewanella oneidensis*. Commun. Biol. 4, 957.

Saunders, S.H., Tse, E.C.M., Yates, M.D., Otero, F.J., Trammell, S.A., Stemp, E.D.A., Barton, J.K., Tender, L.M., Newman, D.K., 2020. Extracellular DNA promotes efficient extracellular electron transfer by pyocyanin in *Pseudomonas aeruginosa* biofilms. Cell 182, 919–932 e19.

Schuetz, B., Schicklberger, M., Kuermann, J., Spormann, A.M., Gescher, J., 2009. Periplasmic electron transfer via the *c*-type cytochromes MtrA and FccA of *Shewanella oneidensis* MR-1. Appl. Environ. Microb. 75, 7789–7796.

Schütz, M.K., Schlegel, M.L., Libert, M., Bildstein, O., 2015. Impact of iron-reducing bacteria on the corrosion rate of carbon steel under simulated geological disposal conditions. Environ. Sci. Technol. 49, 7483–7490.

Shi, L., Chen, B., Wang, Z., Elias, D.A., Mayer, M.U., Gorby, Y.A., Ni, S., Lower, B.H., Kennedy, D.W., Wunschel, D.S., Mottaz, H.M., Marshall, M.J., Hill, E.A., Beliaev, A. S., Zachara, J.M., Fredrickson, J.K., Squier, T.C., 2006. Isolation of a high-affinity functional protein complex between OmcA and MtrC: two outer membrane decaheme *c*-type cytochromes of *Shewanella oneidensis* MR-1. J. Bacteriol. 188, 4705–4714.

Shi, L., Dong, H., Reguera, G., Beyenal, H., Lu, A., Liu, J., Yu, H.Q., Fredrickson, J.K., 2016. Extracellular electron transfer mechanisms between microorganisms and minerals. Nat. Rev. Microbiol. 14, 651–662.

Skovhus, T.L., Eckert, R.B., Rodrigues, E., 2017. Management and control of microbiologically influenced corrosion (MIC) in the oil and gas industry—Overview and a North Sea case study. J. Biotechnol. 256, 31–45.

Tang, H.Y., Holmes, D.E., Ueki, T., Palacios, P.A., Lovley, D.R., 2019. Iron corrosion via direct metal-microbe electron transfer. MBio 10, e00303–e00319.

Tang, H.Y., Yang, C., Ueki, T., Pittman, C.C., Xu, D., Woodard, T.L., Holmes, D.E., Gu, T., Wang, F., Lovley, D.R., 2021. Stainless steel corrosion via direct iron-to-microbe electron transfer by *Geobacter* species. ISME J 15, 3084–3093.

Teal, T.K., Lies, D.P., Wold, B.J., Newman, D.K., 2006. Spatiometabolic stratification of *Shewanella oneidensis* biofilms. Appl. Environ. Microb. 72, 7324–7330.

Turick, C.E., Tisa, L.S., Frank Caccavo, J., 2002. Melanin production and use as a soluble electron shuttle for Fe(III) oxide reduction and as a terminal electron acceptor by *Shewanella algae* BrY. Appl. Environ. Microbiol. 68, 2436–2444.

Wang, D., Jia, R., Kumseranee, S., Punpruk, S., Gu, T., 2021. Comparison of 304 and 316 stainless steel microbiologically influenced corrosion by an anaerobic oilfield biofilm consortium. Eng. Fail. Anal. 122, 105275.

Wang, H., Ju, L.K., Castaneda, H., Cheng, G., Zhang Newby, B., 2014. Corrosion of carbon steel C1010 in the presence of iron oxidizing bacteria *Acidithiobacillus ferrooxidans*. Corros. Sci. 89, 250–257.

Windt, W.D., Boon, N., Siciliano, S.D., Verstraete, W., 2003. Cell density related H_2 consumption in relation to anoxic Fe(0) corrosion and precipitation of corrosion products by *Shewanella oneidensis* MR-1. Environ. Microbiol. 5, 1192–1202.

Wu, M., Wang, T., Wu, K., Kan, L., 2020. Microbiologically induced corrosion of concrete in sewer structures: a review of the mechanisms and phenomena. Constr. Build. Mater. 239, 117813.

Wurzler, N., Schutter, J.D., Wagner, R., Dimper, M., Lützenkirchen-Hecht, D., Ozcan, O., 2020. Abundance of Fe(III) during cultivation affects the microbiologically influenced corrosion (MIC) behaviour of iron reducing bacteria *Shewanella putrefaciens*. Corros. Sci. 174, 108855.

Xia, J., Yang, C., Xu, D., Sun, D., Nan, L., Sun, Z., Li, Q., Gu, T., Yang, K., 2015. Laboratory investigation of the microbiologically influenced corrosion (MIC) resistance of a novel Cu-bearing 2205 duplex stainless steel in the presence of an aerobic marine *Pseudomonas aeruginosa* biofilm. Biofouling 31, 481–492.

Xie, Q., Lu, Y., Tang, L., Zeng, G., Yang, Z., Fan, C., Wang, J., Atashgahi, S., 2021. The mechanism and application of bidirectional extracellular electron transport in the field of energy and environment. Crit. Rev. Env. Sci. Tec. 51, 1924–1969.

Xu, S., Jangir, Y., El-Naggar, M.Y., 2016. Disentangling the roles of free and cytochrome-bound flavins in extracellular electron transport from *Shewanella oneidensis* MR-1. Electrochim. Acta 198, 49–55.

Yang, Y., Masoumeh, M., Zhou, E., Liu, D., Song, Y., Xu, D., Wang, F., Smith, J.A., 2021. *Streptococcus* mutans biofilms induce metabolite-mediated corrosion of 316 L stainless steel in a simulated oral environment. Corros. Sci. 182, 109286.

Yue, Y., Lv, M., Du, M., 2019. The corrosion behavior and mechanism of X65 steel induced by iron-oxidizing bacteria in the seawater environment. Mater. Corros. 70, 1852–1861.

Zhang, P., Xu, D., Li, Y., Yang, K., Gu, T., 2015. Electron mediators accelerate the microbiologically influenced corrosion of 304 stainless steel by the *Desulfovibrio vulgaris* biofilm. Bioelectrochemistry 101, 14–21.

Zhang, Y., He, J., Zheng, L., Jin, Z., Liu, H., Gao, Z., Meng, G., Liu, H., Liu, H., 2022. Corrosion of aluminum alloy 7075 induced by marine *Aspergillus terreus* with continued organic carbon starvation. npj Mater. Degrad. 6, 27.

Zhao, Y., Zhou, E., Xu, D., Yang, Y., Zhao, Y., Zhang, T., Gu, T., Yang, K., Wang, F., 2018. Laboratory investigation of microbiologically influenced corrosion of 2205 duplex stainless steel by marine *Pseudomonas aeruginosa* biofilm using electrochemical noise. Corros Sci 143, 281–291.

Zhou, E., Lekbach, Y., Gu, T., Xu, D., 2022. Bioenergetics and extracellular electron transfer in microbial fuel cells and microbial corrosion. Curr. Opin. Electroche. 31, 100830.